CNS Neuroscience & Therapeutics

ORIGINAL ARTICLE

CNS Neuroscience & Therapeutics

AJAP1 is Dysregulated at an Early Stage of Gliomagenesis and Suppresses Invasion Through Cytoskeleton Reorganization

Lei Han,[1,2,3,4] Kai-Liang Zhang,[1,2,3,4] Jun-Xia Zhang,[5] Liang Zeng,[6] Chun-Hui Di,[6] Brian E. Fee,[6,7] Miriam Rivas,[6,7] Zhao-Shi Bao,[8] Tao Jiang,[8] Darrell Bigner,[9] Chun-Sheng Kang[1,2,3,4,6] & David Cory Adamson[6,7]

1 Department of Neurosurgery, Tianjin Medical University General Hospital, Tianjin, China
2 Tianjin Neurological Institute, Tianjin, China
3 Key Laboratory of Post-trauma Neuro-repair and Regeneration in Central Nervous System, Ministry of Education, Tianjin, China
4 Tianjin Key Laboratory of Injuries, Variations and Regeneration of Nervous System, Tianjin, China
5 Department of Neurosurgery, the First Affiliated Hospital of Nanjing Medical University, Nanjing, China
6 Departments of Surgery and Neurobiology, Preston Robert Tisch Brain Tumor Center, Duke University Medical Center, Durham, NC, USA
7 Durham VA Medical Center, Durham, NC, USA
8 Department of Neurosurgery, Tiantan Hospital, Capital Medical University, Beijing, China
9 Departments of Pathology, Preston Robert Tisch Brain Tumor Center, Duke University Medical Center, Durham, NC, USA

Keywords
AJAP1; Cytoskeleton; Glioma; Invasion; Proliferation.

Correspondence
Chun-Sheng Kang, Ph.D., Laboratory of Neuro-Oncology, Tianjin Neurological Institute, 154, Anshan Road, Heping, Tianjin 300052, China.
Tel.: +86-22-60817499;
Fax: +86-22-27813550;
E-mail: kang97061@gmail.com
and
David Cory Adamson, Duke University Medical Center, Department of Surgery, DUMC Box 2624, 421-MSRB1, Research Drive, Durham, North Carolina, 27710, USA.
Tel.: +919-479-4120;
Fax: +919-479-3287;
E-mail: cory.adamson@duke.edu
Received 24 July 2013; revision 6 January 2014; accepted 7 January 2014

doi: 10.1111/cns.12232

The first two authors contributed equally to this work.

SUMMARY

Aims: Down-regulation of AJAP1 in glioblastoma multiforme (GBM) has been reported. However, the expression profiles of AJAP1 in gliomas and the underlying mechanisms of AJAP1 function on invasion are still poorly understood. **Methods:** The gene profiles of AJAP1 in glioma patients were studied among four independent cohorts. Confocal imaging was used to analyze the AJAP1 localization. After AJAP1 overexpression in GBM cell lines, cellular polarity, cytoskeleton distribution, and antitumor effect were investigated *in vitro* and *in vivo*. **Results:** AJAP1 expression was significantly decreased in gliomas compared with normal brain in REMBRANDT and CGCA cohorts. Additionally, low AJAP1 expression was associated with worse survival in GBMs in REMBRANDT and TCGA U133A cohorts and was significantly associated with classical and mesenchymal subtypes of GBMs among four cohorts. Confocal imaging indicated AJAP1 localized in cell membranes in low-grade gliomas and AJAP1-overexpressing GBM cells, but difficult to assess in high-grade gliomas due to its absence. AJAP1 overexpression altered the cytoskeleton and cellular polarity *in vitro* and inhibited the tumor growth *in vivo*. **Conclusions:** AJAP1 is dysregulated at an early stage of gliomagenesis and may suppress glioma cell invasion and proliferation, which suggests that AJAP1 may be a potential diagnostic and prognostic marker for gliomas.

Introduction

Gliomas are the most common primary tumors in the central nervous system. Malignant glioblastoma multiforme (GBM), World Health Organization (WHO) grade IV, has a median survival of only 12–15 months [1]. Currently, resection of all enhancing tumor with adjuvant chemo- and radiotherapies is the standard of care but provides limited benefit. Target therapies are hypothesized to be the future of more efficacious treatments. Recent clinical trials indicate that an increased survival in recurrent GBM is observed with combined targeting therapies in addition to standard therapy [2]. Experimental studies suggest that some targeted agents may target various tumor behaviors such as reducing angiogenesis, inducing hypoxia, and inhibiting tumor invasion

[3]. Understanding gliomagenesis and malignant progression, which are essential for inhibiting cancer invasion, will contribute to the identity of novel biomarkers and therapeutic targets in glioma therapy.

Accumulating evidence indicates the existence of tumor suppressor-like genes encoded on the 1p36 region [4]. 1p36 genes, including *CHD5*, *CAMTA1*, *KIF1B*, *CASZ1*, and *miR-34a*, demonstrate loss of heterozygosity (LOH), mutation, and homozygous deletion in astrocytomas and oligodendrogliomas [5]. Recent investigations have reported adherens junctional associated protein-1 (*AJAP1*, also known as *Shrew1*) as another tumor suppressor-like gene on chromosome 1 in the 1p36 region. It is frequently deleted or epigenetically silenced in oligodendrogliomas and GBMs [6,7]. Radlwimmer's group carried out comparative genomic hybridization and microarray analysis of spheroid cultures from GBM patients, where *AJAP1*, *EMP3*, and *PDPN* were first described as biomarkers associated with GBM outcome [8]. Subsequently, Zhang and his colleagues demonstrated that *AJAP1* promoter was highly methylated in a wide spectrum of cell lines, and the expression was associated with survival in gliomas [9]. We and others also demonstrated that the *AJAP1* promoter was highly methylated in a wide spectrum of glioma cell lines, and the loss of expression was associated with poorer survival in glioma patients [7].

AJAP1 has been suggested to interact with the E-cadherin–catenin complex in polarized MCF7 and Madin-Darby canine kidney cells [10]; however, AJAP1 does not appear to interact with the N-cadherin complex in nonpolarized epithelial cells [11]. Additionally, CD147 was shown to interact with *AJAP1* and regulate cell invasion [10]. Recently, researcher demonstrated that overexpression of *AJAP1* could suppress cell invasion and migration in GBM cell lines [9]. However, the altered expression profiles of *AJAP1* in gliomas as well as the underlying mechanisms of *AJAP1* on glial cell invasion and proliferation are still poorly understood. In this study, we profiled the expression of *AJAP1* in four independent patient cohorts that came from North American and Chinese populations. Cellular distribution of F-actin in the context of different components of the extracellular compartment matrix (ECM) was investigated *in vitro*, and its antitumor effect was tested *in vitro* and *in vivo*.

Materials and methods

Patients, Microarray Data, and Statistical Analysis

A total of four large gene expression-profiling cohorts of glioma patients were used in this study. REMBRANDT is a robust bioinformatics knowledgebase framework that leverages data warehousing technology to host and integrate clinical and functional genomics data from clinical trials involving 408 patients suffering from gliomas (https://caintegrator.nci.nih.gov/rembrandt) [12]. 408 gliomas are graded in the REMBRANDT database, with 225 GBMs, along with survival information for 188 of the GBMs. Another independent cohort consists of 220 glioma samples collected from the Chinese Glioma Genome Atlas (CGGA, http://www.cgcg.org.cn) [13–15]. Gene expression data from TCGA (data sets: AffyU133a has 558 GBM samples, and AgilentG4502A_07_2 has 483 GBM samples) were downloaded from the UCSC Cancer website (https://genome-cancer.ucsc.edu/proj/site/hgHeatmap/). Within the two TCGA data sets, subtype information is available in 548 and 434 GBMs, and survival information is available in 520 and 428 GBMs, respectively. Kaplan–Meier survival analysis was used to estimate survival distributions, and a log-rank test was used to assess the statistical significance between stratified survival groups, using GraphPad Prism 5.0 statistical software (GraphPad Software, Inc., La Jolla, CA, USA).

Cell Culture and Gene Transfection

Glioma cell lines (U87, U251, D409) were maintained in Improved MEM Zinc Option Medium (Invitrogen) supplemented with 10% FBS at 37°C, 5% CO_2. The *AJAP1* cDNA was isolated from normal cortex by PCR and subcloned into the pEGFP-N1 expression plasmid [7]. The pAJAP1-EGFP expression plasmid was transfected with Lipofectamine 2000 (Invitrogen, Grand Island, NY, USA) and selected by G418 for 10–12 weeks to obtain stable clones for further analysis.

Immunofluorescence for Cultured Cells and Paraffin-embedded Tissue Array

Cells were passaged on glass coverslips (poly-L-lysine or poly-L-lysine/laminin; BD Biosciences, Bedford, MA, USA) overnight to 70% confluence. Coverslips with cells were fixed by formalin solution (neutral buffered, 10% v/v; Sigma-Aldrich, St. Louis, MO, USA) for 10 min. Coverslips were then rinsed twice in phosphate-buffered saline (PBS), pH 7.4, and incubated for 10 min in blocking solution (1% bovine serum albumin in PBS) before antibody incubation. Primary antibodies were AJAP1 (1:200; Sigma), F-actin (1 unit/slide; Invitrogen), and β-tubulin (1:200; Invitrogen). The slides were then incubated in the appropriate antibodies in antibody dilution buffer overnight at 4°C. Secondary antibodies at 1:400 dilution such as Alexo Fluor 566, TexasRed 588, or Alexo Fluor 633 (Invitrogen) were used. Cells were counterstained with mounting media containing DAPI overnight at 4°C and analyzed by Zeiss 780 at 63X. Fluorescence images were acquired by Zen software and analyzed in ImageJ (National Institutes of Health [NIH], Bethesda, MA, USA).

Tissue array slides were fixed in formalin, routinely processed, and paraffin-embedded. Slides were heated for 2 h, then deparaffinized twice in xylene. 1% trypsin was used for epitope unmasking. Slides were incubated for 10 min in blocking solution, then incubated with AJAP1 antibody overnight at 4°C. Secondary antibodies at 1:400 dilutions such as TexasRed 588 were used to detect the expression of AJAP1. Cells were analyzed by Zeiss 780 and analyzed in ImageJ.

Immunohistochemistry for Paraffin-embedded Tissue Array

Primary tumors from 65 patients diagnosed with WHO II (n = 15), WHO III (n = 8), and WHO IV (n = 42) were investigated in this study per IRB-approved protocol, which were col-

lected from Tiantan Hospital from January 2006 through June 2006. Patients were followed using clinical and laboratory monitoring on a regular basis starting at definitive diagnosis. Immunostaining was performed on paraffin sections of tumor specimens by the avidin–biotin complex (ABC) method, as previously described [16]. Sections with no labeling or with fewer than 5% labeled cells were scored as 0. Sections with 5–30% of cells labeled were scored as 1, with 31–70% of cells labeled as 2, and with labeling of ≥71% as 3. The staining intensity was scored similarly, with 0 used for negative staining, 1 for weakly positive, 2 for moderately positive, and 3 for strongly positive. The scores for the percentage of positive tumor cells and for the staining intensity were added to generate an immunoreactive score for each specimen. The product of the quantity and intensity scores was calculated such that a final score of 0–1 indicated negative expression, 2–3 indicated weak expression, 4–5 indicated moderate expression, and 6 indicated strong expression. Each sample core was individually analyzed using the NIH Image J (v1.42) plug-in deconvolTMA. Cases with discrepancies in the scores were discussed to reach a consensus.

Western Blot, Transwell, and Colony Formation Assay

Western blot, transwell, and colony formation assays were performed as previously described [17].

Nude Mouse Glioma Intracranial Model and AJAP1 Treatment

U87 cells were co-transfected with DOX-inducible *AJAP1* recombinant adenovirus (SinoGenoMax, Beijing, China) and luciferase lentivirus (GenePharma, Shanghai, China) *in vitro* for 2 days. After confirmation of DOX-induced expression of *AJAP1* (data not shown), 500,000 cells in suspension were injected stereotactically into the brain of 5-week-old BALB/c-nu mice [18]. The mice were treated with 2 mg/mL freshly prepared DOX (Santa Cruz, Dallas, TX, USA) in drinking water. Sucrose (5%) was added to decrease the bitter taste of DOX water. A red bottle was used to prevent light-induced DOX degradation, and water was replaced twice weekly. Tumor growth was monitored by fluorescent images of whole mice using an IVIS Lumina Imaging System (Xenogen, Waltham, MA, USA) every 10 days until 30 days. The mice were anesthetized, injected intraperitoneally with 50 mg/mL of D-luciferin (Promega, Madison, WI, USA), and imaged with the IVIS Imaging System for 5–10 min. Additionally, the body weight and overall survival time of mice were also monitored. Paraffin-embedded sections (5 μm) were stained with hematoxylin and eosin and used for immunofluorescence stain.

Statistical Analysis

Significance analysis of microarrays (SAM, FDR < 0.05, q value < 0.05) was used to identify significant genes. Kaplan–Meier survival analysis was used to estimate the survival distributions, and the log-rank test was used to assess the statistical significance between stratified survival groups using the median value as the cutoff. One-way ANOVA, Student's t-test, and the Pearson correlation were used to determine significant differences. All data are presented as the mean ± standard error. A two-sided P value of <0.05 was regarded as significant.

Results

Gene Profiling Identifies Down-regulation of AJAP1 in Early Stage of Gliomagenesis

To investigate the expression profile of *AJAP1* in normal brain and gliomas, the REMBRANDT cohort, which includes 21 normal brains and 408 gliomas, was the first to be employed. In 408 gliomas, 99 (24.3%) were WHO II, 84 (20.6%) were WHO III, and 225 (55.1%) were WHO IV. *AJAP1* was found to be significantly down-regulated in all glioma patients, compared with normal brain ($P < 0.01$, Figure 1A, left). However, *AJAP1* expression in WHO II was not significantly different between WHO III and WHO IV (Figure 1A, left), indicating that loss of expression of *AJAP1* might be an early event in gliomagenesis. To further investigate the role of *AJAP1* in GBM survival, we compared *AJAP1* expression and overall survival using Kaplan–Meier survival curve analysis with a log-rank comparison. Overall survival was significantly associated with the expression level of *AJAP1* ($P = 0.027$, top 30% vs. bottom 30%, Figure 1A, right, 188 cases).

To further verify *AJAP1* expression across normal brain and gliomas with each WHO grade, we also conducted similar analysis for the 220 patients with gliomas in the CGCA cohort, in which 84 (38.2%), 47 (21.4%), and 89 (40.4%) patients received a diagnosis of WHO II, WHO III, and WHO IV, respectively. These results were consistent with the findings from the REMBRANDT cohort, but with a mild difference between WHO III and WHO IV ($P = 0.0425$, Figure 1B, left, 87 cases). Surprisingly, insignificance was observed between overall survival and the expression levels of *AJAP1* by top 30% versus bottom 30% ($P = 0.6888$, Figure 1B, right). To clarify the impact of *AJAP1* expression on overall survival in GBMs, two TCGA cohorts with 948 cases were used. As shown in Figure 1C,D, inconsistent results for top 30% versus bottom 30% were observed in the two TCGA cohorts, one approached significance ($P = 0.0810$, Figure 1C, 520 cases) and the other was statistically significant ($P = 0.0316$, Figure 1D, 428 cases). These findings, which suggest *AJAP1* might be associated with overall survival in GBM, provide provocative evidence that loss of expression of *AJAP1* is involved in initial gliomagenesis and remains decreased in expression in higher grades of gliomas.

AJAP1 is Down-regulated in Classical and Mesenchymal Subtype of GBMs

Four molecular subtypes, that is, classical, mesenchymal, neural, and proneural subtypes, were first described by TCGA in 2010 in GBM [19]. To address whether *AJAP1* expression might distinguish among GBM subtypes, we applied the TCGA classification system to the REMBRANDT, CGCA, and TCGA data and annotated the samples according to the TCGA four subtypes using the Prediction Analysis of Microarrays classifier as previously described [19]. One-way ANOVA indicated a significant difference in *AJAP1* expression between the four GBM subtypes in the four cohorts. *AJAP1* expression in the classical or mesenchymal sub-

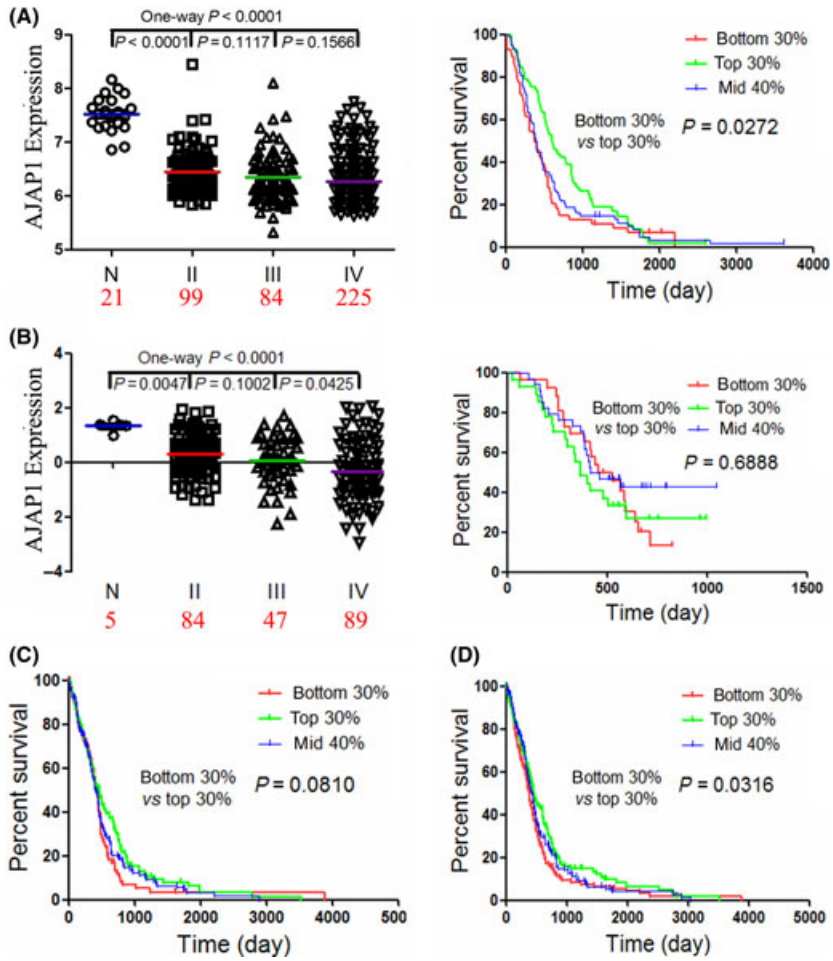

Figure 1 Down-regulation of *AJAP1* in early stage of gliomagenesis. The expression of *AJAP1* was detected in both REMBRANDT (**A**) and CGCA (**B**) cohorts. *AJAP1* was significantly down-regulated in WHO II glioma patients, compared with normal brain ($P < 0.001$). Kaplan–Meier survival curve was used to examine the function of *AJAP1* expression profile on the survival of GBM patients. (**C**–**D**) Kaplan–Meier survival curve analysis was used to study the impact of *AJAP1* on the overall survival in GBM patients selected from two TCGA cohorts.

types was much lower than that in the neural subtypes in all four data sets (Figure 2A–D). Additionally, *AJAP1* expression in the classical or mesenchymal subtypes was also lower than in the proneural subtype, but only in the TCGA cohorts (Figure 2C,D). The classical and mesenchymal subtype-specific expression of *AJAP1* in GBMs, which was consistent among the four cohorts, suggested that *AJAP1* might be involved in the clinical prognosis and therapeutic response of specific subtypes of GBMs.

Expression and Localization of AJAP1 in Human Glioma Samples

In the present study, 15 diffuse astrocytomas (WHO II), 8 anaplastic oligodendrogliomas (WHO III), and 42 glioblastoma (WHO IV) tissues were prepared in a tissue array to characterize *AJAP1* expression. In WHO II astrocytomas, AJAP1 was expressed in 80.0% (8/10) of cases (Figure 3A). There was a significant decrease in AJAP1 expression in high-grade cases (WHO III and WHO IV), compared to low-grade cases (WHO II) (Figure 3A bottom, $P < 0.0001$). Of note, AJAP1 was present only in the cell membrane in WHO II cases, which was clearer at higher magnification (Figure 3B). On the other hand, less AJAP1 could be detected in almost two-thirds of WHO IV cases (Figure 3C).

To further confirm subcellular localization of AJAP1 in gliomas, we created an EGFP-AJAP1 fusion construct and established stable-transfected U87 cells as previously described [7]. As shown in Figure 3D, AJAP1 (red) clearly localized along the cell membrane. GFP (green) co-localized exactly with AJAP1, resulting in yellow signal after merged with AJAP1 (red).

Restoration of AJAP1 Alters Growth Pattern and Reorganizes Cytoskeleton in GBM Cells *In vitro*

We previously examined *AJAP1* expression in 12 primary GBM samples, eight glioma cell lines, and four normal brain samples with qPCR, which proved that U87 GBM cell was absent of *AJAP1* expression [7]. After stable transfection of *AJAP1* in U87 cells (U87-AJAP1), cell growth patterns and organization of the cytoskeleton were assessed by confocal microscopy (EGFP-vector transfected U87 cell [U87-vector] was a negative control).

As indicated in Figure 4A, after growth to 80% confluence *in vitro*, U87-vector cells formed a spheroid-like growth pattern, which was clearly demonstrated in low magnification. After co-staining with fluorescent phalloidin for F-actin and Alexa-Fluro 633 for β-tubulin, U87-vector spheroid-like clusters under low magnification displayed strong signal in the central area of cell clusters both for F-actin and for β-tubulin (Figure 4A). In U87-vector group,

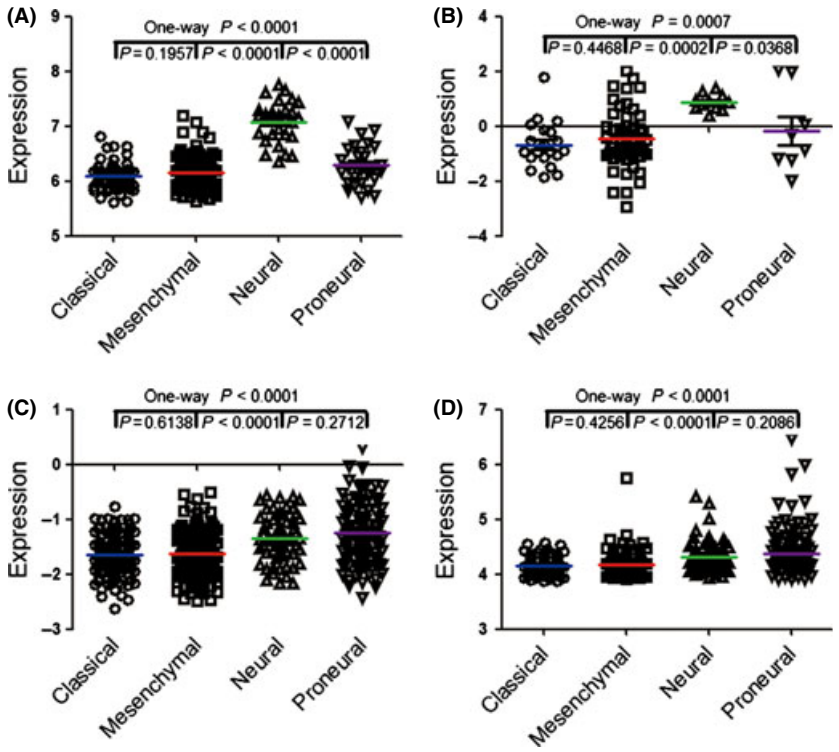

Figure 2 Down-regulation of *AJAP1* is consistent in classical and mesenchymal GBM. The REMBRANDT with 225 GBM cases (**A**), CGCA with 89 GBM cases (**B**), TCGA AgilentG4502A_07_2 with 548 GBM cases (**C**), and TCGA AffyU133a with 225 GBM cases (**D**) cohorts were applied to the classification system, and the expression of *AJAP1* was detected to be down-regulated in classical and mesenchymal subtypes compared with the other two types.

outwardly elongating cells at the periphery of cell clusters extended long projections into surroundings that were F-actin and β-tubulin positive under high magnification (Figure 4B). These projections (filopodia) were not prominent on U87-AJAP1 group. Filopodia projections distributed in the protrusion of cell clusters periphery possibly represent cells migrating into surroundings. Filopodia projections were even more prominent when U87-vector cells were grown on laminin-/polylysine-double-precoated cover slides (Figure 4C,D). Next, we asked whether restoration of *AJAP1* might alter the growth pattern and distribution of cytoskeleton components. U87-AJAP1 cells were unable to form spheroid-like cell clusters under low magnification; however, the U87-AJAP1 cells were changed into a more round-like morphology with fewer protrusions (Figure 4A,B). Moreover, F-actin staining indicated the formation of lamellipodia (more broad sheet-like extensions) and disappearance of filopodia in U87-AJAP1 cells (Figure 4B), which is more prominent on laminin-/polylysine-double-precoated cover slides (Figure 4C,D). U251-vector and D409-vector cells had more lamellipodia than U87-vector (Figure 4E,F compared to A). Nevertheless, *AJAP1* overexpression appeared to also decrease the number of lamellipodia in U251 and D409 as well (Figure 4E,F, bottom panels compared to top panels).

AJAP1 Overexpression Inhibits Glioma Cell Proliferation and Invasion *In vitro* and *In vivo*

Overexpression of AJAP1 in U87 cells resulted in a marked decrease in cell proliferation and invasion through colony formation and transwell assays as compared with the same cell type transfected with pvector (Figure 5A,B). Next, we explored expression changes in proliferation and invasion proteins. Western blot assays revealed that AJAP1 overexpression triggered a reduction in MMP9 and Ki67 expression (Figure 5C).

To further evaluate the functional significance of *AJAP1* overexpression on glioma development, we employed a glioma xenograft model with U87 cells. To monitor treatment responses in live animals, U87 cells were first engineered to stably express firefly luciferase prior to intracranial implantation in mice, in addition to rAd-AJAP1. Bioluminescent imaging showed tumor growth status in each treated group. The rAd-AJAP1 mice treated with DOX displayed a marked reduction in the tumor growth compared to the control group (rAd-AJAP1 group without DOX) (Figure 6A,B). Moreover, in accordance with the bioluminescent imaging results, immunohistochemical analysis revealed a DOX treatment-dependent reduction in tumor growth (Figure 6C). The rAd-AJAP1 group treated with DOX exhibited body weight loss from only during the later stage of the experiment. In contrast, animals in the control group exhibited progressive body weight loss from the early stages of the experiment due to advanced disease (Figure 6D). A survival curve demonstrated that *AJAP1* overexpression could significantly increase the survival time of mice as compared with control group (Figure 6E). These data indicate that overexpression of AJAP1 in *vivo* functions similarly as that *in vitro* [7].

Next we examined whether the strict regulation of *AJAP1* expression also occurs in animal model. High levels of EGFP and AJAP1 expression were induced in tumor tissue from the mice treated with Dox for 20 days, whereas low EGFP and AJAP1

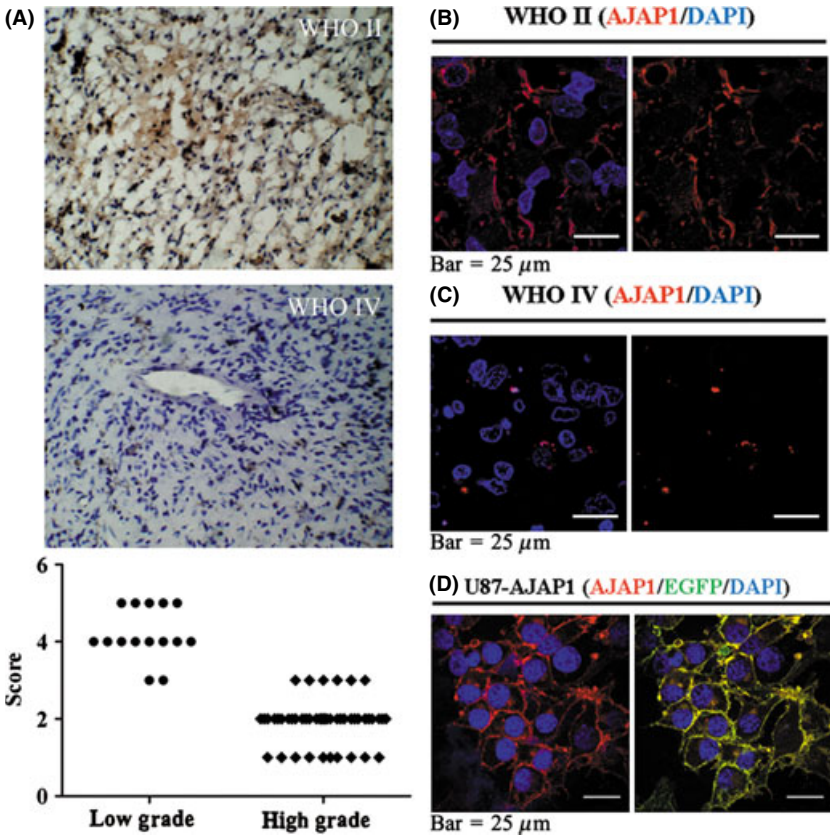

Figure 3 Expression and localization of AJAP1 in surgical samples and glioma cells. (**A**) Primary tumor tissue array from 65 patients diagnosed with WHO II 15 cases, WHO III 8 cases, and WHO IV 42 cases was prepared, and immunohistochemistry was introduced to detect the expression of AJAP1. U87 glioma cells were infected with *AJAP1* plasmid to obtain U87 cells stably expressing *AJAP1*. Immunofluorescence analysis was used to examine the localization of AJAP1 in surgical samples (**B**, **C**) and U87 cells with stable expressing AJAP1 (**D**).

expression was detected in tumor from the mice not treated with Dox (Figure 6F). These results indicate that the induction of *AJAP1* expression by the Dox-inducible system is strictly controlled in intracranial U87 tumor-bearing mice.

Discussion

Uncontrolled proliferation and invasive growth are the fundamental hallmarks of epithelial cancers [20]. It is well known that epithelial cancers, including GBM, present with highly invasive growth patterns. Invasion of surrounding parenchyma precludes complete pathologically total resection and thereby results in recurrence from these tumors [21]. Thus, identifying new biomarkers and therapeutic targets becomes urgent. In the present study, we firstly analyzed the expression of *AJAP1* in the top four independent cohorts from North American and Chinese populations. Additionally, the TCGA subtype classifications were employed for GBM. Our results demonstrated a significantly decreased expression of *AJAP1* in WHO II gliomas compared with that in normal brains. Similarly to WHO II gliomas, the expression of *AJAP1* displayed a significant decrease in high-grade gliomas (WHO III and WHO IV). In survival analyses, cross-validation from REMBRANDT and TCGA Agilent cohorts identified *AJAP1* as a significant biomarker in GBM outcome. GBMs in the bottom 30% of *AJAP1* expression had a shorter overall survival time (Figure 1). These findings, together with robust decrease in expression in WHO II, strongly imply that loss of *AJAP1* expression most likely occurs in an early stage of gliomagenesis and is continuously down-expressed in high-grade gliomas. It remains unclear whether *AJAP1* expression acts as a key driver in gliomagenesis or merely supports it.

To further understand the translational implications of *AJAP1* in GBM, we analyzed *AJAP1* expression in four subtypes according to current TCGA classifications. We found that *AJAP1* was significantly lower in classical and mesenchymal subtypes, compared with neuronal and proneural subtypes in all four cohorts. To the best of our knowledge, this is the first study that looks at the direct linkage between *AJAP1* expression and TCGA subtype classifications in human GBM. Most WHO grade III gliomas as well as 75% of lower-grade gliomas from the validation sets in the TCGA data sets were classified as proneural or neural. The lower expression of *AJAP1* in classical and mesenchymal suggests that expression of *AJAP1* in GBM might inhibit gliomagenesis in these less frequent subtypes (Figure 2). In the TCGA study, intensive treatment was defined as concurrent chemo- and radiotherapy or more than three subsequent cycles of chemotherapy. Survival analysis indicated that intensive therapy could benefit patient survival in classical and mesenchymal subtypes, which suggests that *AJAP1* might be a potential biomarker to predict therapeutic response in GBM. The mechanisms of *AJAP1* sensitization to chemotherapy (e.g., temozolomide) or radiotherapy warrant further study.

Dysregulation of *AJAP1* expression has been reported in other cancer types. Zhang et al. reported approximately 640-kb deletion in 1p that contained *AJAP1* in 177 oligodendroglioma samples. This is the first evidence that connected *AJAP1* to gliomas. Meanwhile, they demonstrated that restoration of *AJAP1* in U251 GBM

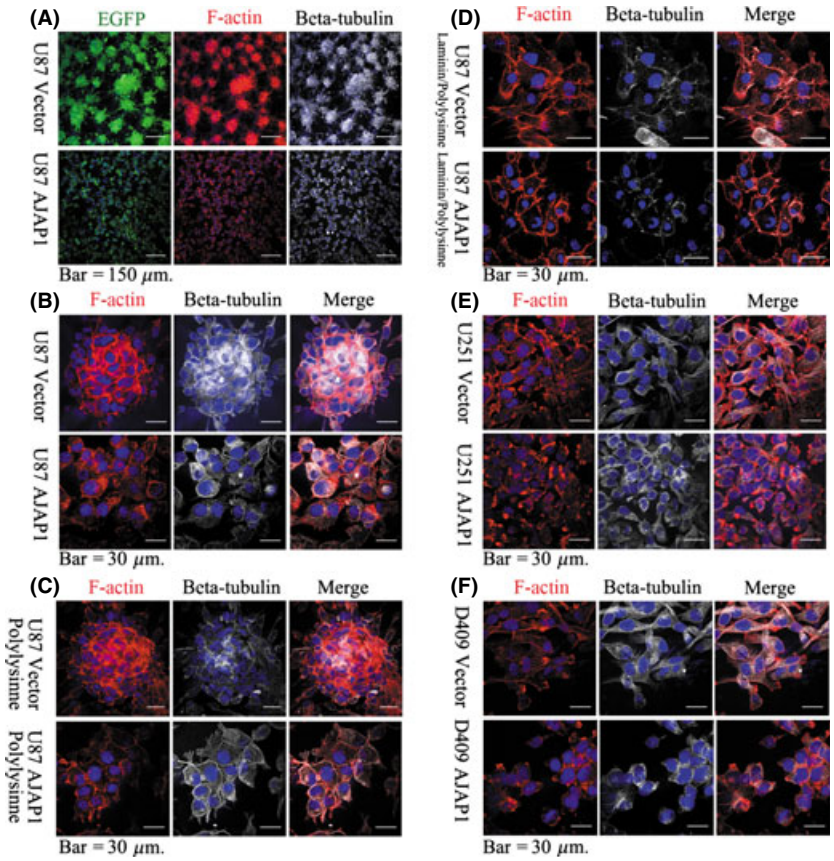

Figure 4 Overexpression of *AJAP1* alters growth pattern and reorganizes cytoskeleton in GBM cells. (**A**) U87 cells were infected with vector or AJAP1 plasmid. 48 to 72 h after incubation, confocal assay was used to examine the growth pattern. (**B**) U87 vector cells and U87-AJAP1 cells were stained with F-actin and β-tubulin to detect the filopodia distribution. DAPI was used to mark the nuclei. (**C**, **D**) AJAP1 depolarized glioma cell in different ECMs. U87 glioma cells were infected with or without AJAP-1. 48 h after infection, round-like morphology with fewer protrusions accompanied with larger lamellipodia could be seen in AJAP1-transfected cells. U251 (**E**) and D409 (**F**) glioma cells were infected with vector or AJAP1 plasmid; F-actin and β-tubulin were stained to examine the filopodia or lamellipodia distribution.

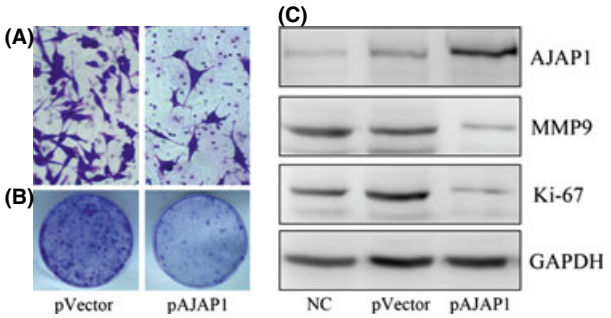

Figure 5 Overexpression of *AJAP1* suppresses proliferation and invasion in U87 cells. (**A**) U87 cells were transfected with pvector or pAJAP1 plasmid. 48 to 72 h after transfection, transwell assay was used to examine the invasive ability. (**B**) U87 cells were transfected with pvector or pAJAP1 plasmid. 48 to 72 h after transfection, colony assay was used to examine the proliferation. (**C**) Proteins related to proliferation and invasion were tested after overexpressing AJAP1 in U87 glioma cells.

cells could result in inhibition of cell adhesion and migration [6]. Our previous study indicated that loss of expression of *AJAP1* was found in more than 80% of primary GBM, and the loss of expression correlated with *AJAP1* methylation. Suppression of migration in D409 GBM cells was also observed. In the present study, we constructed the *AJAP1* expression plasmid and the Dox-inducible recombinant adenovirus expression system for restoration of *AJAP1 in vitro* and *in vivo*. Confocal imaging demonstrated that cell growth patterns, cell morphology, and cellular distribution of F-actin and β-tubulin changed in *AJAP1* stable-transfected GBM cells (Figure 4). AJAP1 has been associated with E-cadherin-mediated adherens junctions by interacting with the cadherin–catenin complex in polarized cells, which further supports a role for AJAP1 in altering cell morphology in GBM cells [22]. Our study suggests that AJAP1 may also suppress cell invasion and migration through cytoskeleton reorganization, that is, decreasing the filopodia extending processes and changes in β-tubulin distribution. F-actin is a major component of focal adhesion complexes, plays a role in cell adhesion and migration, and facilitates the formation of filopodia. These are essential processes in cell migration because they function as sensors of the external microenvironment and as plasma membrane extensions that form initial contacts with the ECM [23]. Collectively, the decrease in filopodia, increase in lamellipodia, and rearrangement of β-tubulin into a loose cytoskeleton network all suggest a suppressive effect of AJAP1 on cell migration and invasion [24]. Accumulating evidence indicates that many pathways are involved in the regulation of the cytoskeleton network, including G protein-coupled receptors (GPCRs), integrins, receptor tyrosine kinases (RTKs), and numerous other specialized receptors, such as the semaphorin 1a receptor PlexinA. All of these can lead to diverse effects on cell activity, including changes in cell shape, migration, proliferation, and survival [25]. The connections between AJAP1 and the cytoskeleton network are likely complex and need further investigation.

In summary, gene profiling of gliomas showed that dysregulated *AJAP1* exists in the early stage of gliomagenesis. In particular,

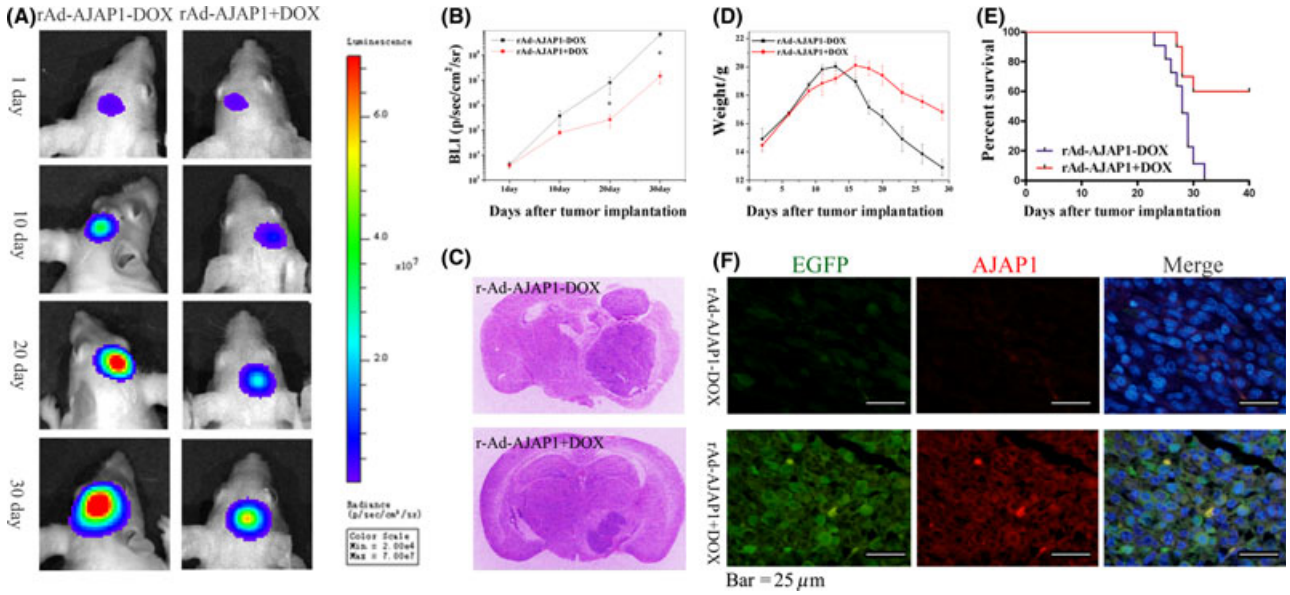

Figure 6 Overexpression of *AJAP1* suppresses tumor growth in orthotopic U87 mice. (**A**, **B**) Bioluminescent images from control and rAd-AJAP1 treated with Dox at 1, 10, 20, and 30 d after tumor implantation. (**C**) Hematoxylin–eosin–saffron staining on representative tumors with and without Dox treatment 20 days after tumor implantation. (**D**) The mice body weights were evaluated. (**E**) Survival curve for all groups of intracranial U87 tumor-bearing mice. (**F**) Dox-dependent AJAP1 and EGFP expression in the tumors from the mice brain after 20-day administration of drinking water containing 0 or 2 mg/mL of Dox.

AJAP1 expression is associated with low and high tumor grades, as well as the clinical outcome of patients with GBMs. Its loss expression predicts poor clinical outcome and may serve as a promising biomarker for intensive therapy, especially in classical and mesenchymal GBM patients. Few studies have investigated the function of AJAP1 and cytoskeleton regulation in gliomas. Further studies are warranted to explore the biological functions of AJAP1 that may improve our understanding of the initiation of gliomas and development of new biomarker and therapeutic target for individualized therapy for GBM.

Acknowledgments

We are grateful to Yasheng Gao (Light Microscopy Core Facility, Duke University) for his assistance with the confocal imaging acquirement. This work was supported by the National High Technology Research and Development Program of China (863 Program) (2012AA02A508), Project supported by Municipal Science & Technology Commission of Tianjin, China (12JCZDJC24300, 12ZCDZSY17300), and the Biomedical Laboratory Research & Development Service of the VA Office of Research and Development (I01BX007080).

Conflict of Interest

The authors declare no conflict of interest.

References

1. Bao ZS, Zhang CB, Wang HJ, et al. Whole-genome mRNA expression profiling identifies functional and prognostic signatures in patients with mesenchymal glioblastoma multiforme. *CNS Neurosci Ther* 2013;**9**:714–720.
2. Yuan Y, Xue X, Guo RB, Sun XL, Hu G. Resveratrol enhances the antitumor effects of temozolomide in glioblastoma via ROS-dependent AMPK-TSC-mTOR signaling pathway. *CNS Neurosci Ther* 2012;**7**:536–546.
3. Shi ZD, Qian XM, Liu CY, et al. Aspirin-/TMZ-coloaded microspheres exert synergistic Antiglioma efficacy via inhibition of β-catenin transactivation. *CNS Neurosci Ther* 2013;**2**:98–108.
4. Henrich KO, Schwab M, Westermann F. 1p36 tumor suppression–a matter of dosage? *Cancer Res* 2012;**23**:6079–6088.
5. Smith JS, Alderete B, Minn Y, et al. Localization of common deletion regions on 1p and 19q in human gliomas and their association with histological subtype. *Oncogene* 1999;**28**:4144–4152.
6. McDonald JM, Dunlap S, Cogdell D, et al. The SHREW1 gene, frequently deleted in oligodendrogliomas, functions to inhibit cell adhesion and migration. *Cancer Biol Ther* 2006;**3**:300–304.
7. Lin N, Di C, Bortoff K, et al. Deletion or epigenetic silencing of AJAP1 on 1p36 in glioblastoma. *Mol Cancer Res* 2012;**2**:208–217.
8. Ernst A, Hofmann S, Ahmadi R, et al. Genomic and expression profiling of glioblastoma stem cell-like spheroid cultures identifies novel tumor-relevant genes associated with survival. *Clin Cancer Res* 2009;**21**:6541–6550.
9. Cogdell D, Chung W, Liu Y, et al. Tumor-associated methylation of the putative tumor suppressor AJAP1 gene and association between decreased AJAP1 expression and shorter survival in patients with glioma. *Chin J Cancer* 2011;**4**:247–253.
10. Schreiner A, Ruonala M, Jakob V, et al. Junction protein shrew-1 influences cell invasion and interacts with invasion-promoting protein CD147. *Mol Biol Cell* 2007;**4**:1272–1281.
11. Bharti S, Handrow-Metzmacher H, Zickenheiner S, Zeitvogel A, Baumann R, Starzinski-Powitz A. Novel membrane protein shrew-1 targets to cadherin-mediated junctions in polarized epithelial cells. *Mol Biol Cell* 2004;**1**:397–406.
12. Madhavan S, Zenklusen JC, Kotliarov Y, Sahni H, Fine HA, Buetow K. Rembrandt: helping personalized medicine become a reality through integrative translational research. *Mol Cancer Res* 2009;**2**:157–167.
13. Yan W, Zhang W, You G, et al. Molecular classification of gliomas based on whole genome gene expression: a

systematic report of 225 samples from the Chinese Glioma Cooperative Group. *Neuro Oncol* 2012;**12**:1432–1440.

14. Lin Y, Chen Y, Wang Y, et al. ZIP4 is a novel molecular marker for glioma. *Neuro Oncol* 2013;**8**:1008–1016.
15. Zhang JX, Zhang J, Yan W, et al. Unique genome-wide map of TCF4 and STAT3 targets using ChIP-seq reveals their association with new molecular subtypes of glioblastoma. *Neuro Oncol* 2013;**3**:279–289.
16. Zhang J, Huang K, Shi Z, et al. High β-catenin/Tcf-4 activity confers glioma progression via direct regulation of AKT2 gene expression. *Neuro Oncol* 2011;**6**:600–609.
17. Zhang KL, Han L, Chen LY, et al. Blockage of a miR-21/EGFR regulatory feedback loop augments anti-EGFR therapy in glioblastomas. *Cancer Lett* 2014;**1**:139–149.
18. Chen L, Han L, Zhang K, et al. VHL regulates the effects of miR-23b on glioma survival and invasion via suppression of HIF-1α/VEGF and β-catenin/Tcf-4 signaling. *Neuro Oncol* 2012;**8**:1026–1036.
19. Bao ZS, Zhang CB, Wang HJ, et al. Whole-genome mRNA expression profiling identifies functional and prognostic signatures in patients with mesenchymal glioblastoma multiforme. *CNS Neurosci Ther* 2013;**19**:714–720.
20. Vancheri C, Failla M, Crimi N, Raghu G. Idiopathic pulmonary fibrosis: a disease with similarities and links to cancer biology. *Eur Respir J* 2010;**3**:496–504.
21. Han L, Yue X, Zhou X, et al. MicroRNA-21 Expression is Regulated by β-catenin/STAT3 pathway and Promotes Glioma Cell Invasion by Direct Targeting RECK. *CNS Neurosci Ther* 2012;**7**:573–583.
22. Gross JC, Schreiner A, Engels K. Starzinski-Powitz A.E-cadherin surface levels in epithelial growth factor-stimulated cells depend on adherens junction protein shrew-1. *Mol Biol Cell* 2009;**15**:3598–3607.
23. Hwang JH, Smith CA, Salhia B, Rutka JT. The role of fascin in the migration and invasiveness of malignant glioma cells. *Neoplasia* 2008;**2**:149–159.
24. Garcia GG, Miller RA. Age-dependent defects in TCR-triggered cytoskeletal rearrangement in CD4+ T cells. *J Immunol* 2002;**9**:5021–5027.
25. Aplin AE, Juliano RL. Integrin and cytoskeletal regulation of growth factor signaling to the MAP kinase pathway. *J Cell Sci* 1999;**112**(Pt 5):695–706.